ISSN 0023-1584, Kinetics and Catalysis, 2010, Vol. 51, No. 2, pp. 200–206. © Pleiades Publishing, Ltd., 2010.
Original Russian Text © V.Sh. Aliev, I.A. Badmaeva, 2010, published in Kinetika i Kataliz, 2010, Vol. 51, No. 2, pp. 216–222.

Photopolymerization Kinetics of Monolayer and Bilayer Langmuir–Blodgett Films of Acetylenic Acid Salts

V. Sh. Aliev and I. A. Badmaeva

Institute of Semiconductor Physics, Siberian Branch, Russian Academy of Sciences, Novosibirsk, 630090 Russia
e-mail: aliev@thermo.isp.nsc.ru

Received November 12, 2008

Abstract—The photopolymerization of thin (monolayer and bilayer) Langmuir–Blodgett films of the lead salt of 2-docosynoic acid ($CH_3(CH_2)_{18}C{\equiv}CCOOH$, DCA), with a triple bond near the carboxylic group, and the lead salt of 23-tetracosynoic acid ($HC{\equiv}C(CH_2)_{21}COOH$, TCA), with a triple bond far from the carboxyl group, has been investigated by IR spectroscopy. The principal distinctions between the polymerization kinetics of the DCA salt and that of the TCA salt are observed for bilayers. It is hypothesized that the perfection of the molecular packing in the bilayers is governed by the interlayer interaction of carboxyl groups, which exerts a stronger effect on the mutual orientation of the triple bonds in the DCA salt films as compared to the TCA salt films. A model is suggested for describing the kinetics of the two-dimensional photopolymerization of monoacetylenic compounds. A comparison between simulated and experimental data for the monolayer films demonstrates that the observed saturation of conversion (α) as a function of the UV exposure time (t) at the $\alpha \approx 0.5$–0.6 level can be attributed to the fact that the intermolecular distance lengthens with local film densification during polymerization. The effects of the substrate and the orientation of molecules in the layer on $\alpha(t)$ is reported.

DOI: 10.1134/S0023158410020059

Thin organic films produced by the Langmuir–Blodgett (LB) method are a convenient model object for investigating the physical chemistry of solid-phase topochemical reactions [1] in low-dimensional systems. These reactions include the photopolymerization of lead salts of 23-tetracosynoic acid (TCA) and 2-docosynoic acid (DCA) in LB layers. These compounds can be employed as electron resists in nanolithography with 20–50 nm resolution and in sensors based on conducting ultrathin organic films. Therefore, investigation of their photopolymerization kinetics is of practical significance.

The kinetics of topochemical polymerization is governed by the structure of the molecular crystal and by the mechanism of molecular interaction. Earlier, we studied the structure and photopolymerization kinetics of LB layers of lead, cadmium, and copper salts of TCA and DCA [2–4]. Most of these studies were carried out on multilayer films consisting of 30 LB layers or more. This study is focused on 1- to 3-layer LB films. We established in earlier works [2, 3] that conversion (α) depends on the number of layers in the film: α increases from 0.5 to 0.8 as the number of layers in increased from one to four and remains practically unchanged as the number of layers is further raised. Under the assumption that polymerization in each LB layer is independent of polymerization in adjacent layers, conversion should be independent of the film thickness. The dependence of α on the number of layers can be due to the effect of the substrate on the interlayer molecular interaction. Here, we report studies aimed at understanding why α changes with an increasing number of LB layers.

There is a two-dimensional kinetic model for the photopolymerization of diacetylenic LB films [5, 6], but no kinetic model has been reported for films of monoacetylenic compounds, such as TCA and DCA. Here, we suggest, for analysis of the $\alpha(t)$ dependence, an original model based on numerical integration of the kinetic equation relating the reaction rate to the probability of separate photopolymerization stages occurring at an arbitrary point of time.

EXPERIMENTAL

The synthesis of the starting reagents—TCA and DCA—is described in detail elsewhere [2]. LB films were obtained by forming monolayers on the surface of an aqueous subphase containing a lead salt solution at a concentration of 1×10^{-4} mol/l (pH 5.0) and by transferring these monolayers onto a substrate. The substrates were polished Si(100) wafers. Immediately before film growth, the silicon wafers were treated with an HF solution to remove the natural oxide and to make the surface hydrophobic. Monolayers were transferred onto the substrate at surface pressures of $\pi = 29 \times 10^{-3}$ and 35×10^{-3} N/m and a temperature of 18 ± 1°C with a velocity of 1.5 cm/min. The films had a Y-type structure. The photopolymerization of LB films was carried out in a vacuum chamber at a resid-

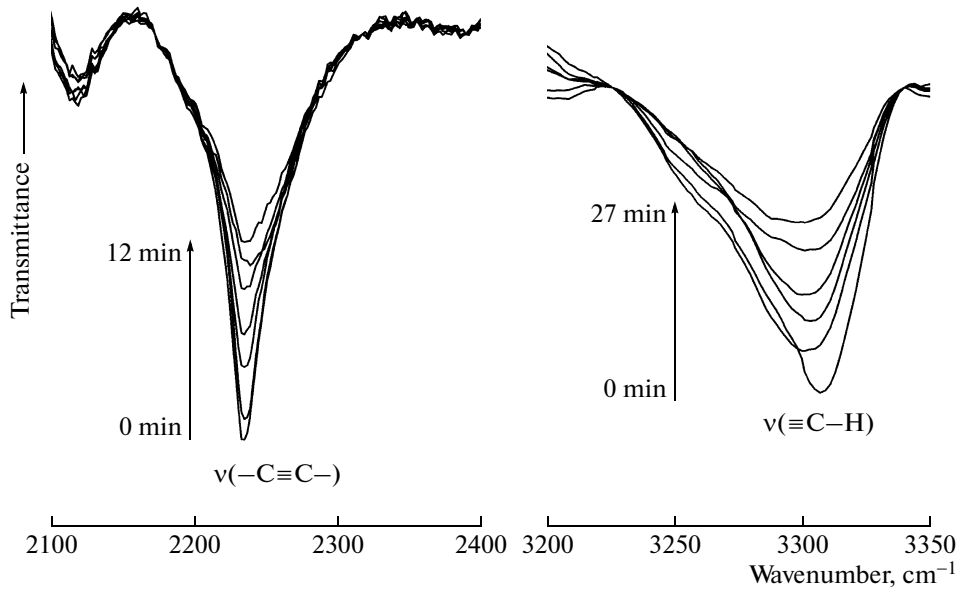

Fig. 1. IR absorption bands due to the stretching vibrations of the C−H bond in the terminal R−C≡C−H group in the bilayer TCA salt film (3310 cm^{-1}) and the stretching vibrations of the C≡C bond in the monolayer DCA salt film (2234 cm^{-1}) at various UV irradiation times.

ual pressure of 10^{-2} Pa. The chamber had a window made from optical quartz KU-1. The samples were irradiated using a DB-15 low-pressure mercury lamp at room temperature. The radiation from the lamp had a discrete spectrum with the most intense bands at 254, 295, 312, 365, 405, 435, 491, 547, 578, and 691 nm. By using a set of optical filters, it was found that polymerization takes place only when the film is irradiated at 254 nm. The intensity of this line measured on the substrate surface in the chamber was 1.7×10^{-3} W/cm^2, which corresponds to a photon flux of 2.18×10^{15} s^{-1} cm^{-2}. The IR spectra of the initial and UV-irradiated films were recorded on a Bruker-IFS-113 Fourier transform spectrophotometer in the range of 1000–500 cm^{-1} (resolution 1 cm^{-1}). The sensitivity of the IR spectrophotometer was enhanced significantly by using the multiple reflection attenuated total reflectance technique [7]. The TCA salt conversion was derived from the area of the peak at 3310 cm^{-1}, which is due to the C−H stretching vibrations in the terminal R−C≡C−H group. The DCA salt conversion was determined from the area of the peak at 2234 cm^{-1}, which corresponds to the C≡C stretching vibrations. The conversion α was calculated as $\alpha(t) = (A_0 - A_R(t))/A_0$, where A_0 and $A_R(t)$ are the peak areas for the initial sample and for the same sample irradiated for time t, respectively.

RESULTS

Figure 1 shows the IR absorption bands that were used to calculate $\alpha(t)$. The $\alpha(t)$ dependences for TCA salt films is plotted in Fig. 2. It is interesting that $\alpha(t)$ for the monolayer and bilayer films is the same. The curve has a sigmoid shape with saturation at $\alpha \sim 0.6$. Figure 3 plots the similar $\alpha(t)$ dependences for monolayer DCA salt films grown at different surface pressures (π). As π is raised, the curve loses its sigmoid shape and the saturation level and initial slope of $\alpha(t)$ increase. For $\pi = 29 \times 10^{-3}$ N/m, we present the data of two independent measurements. The $\alpha(t)$ dependences for monolayer, bilayer, and three-layer DCA

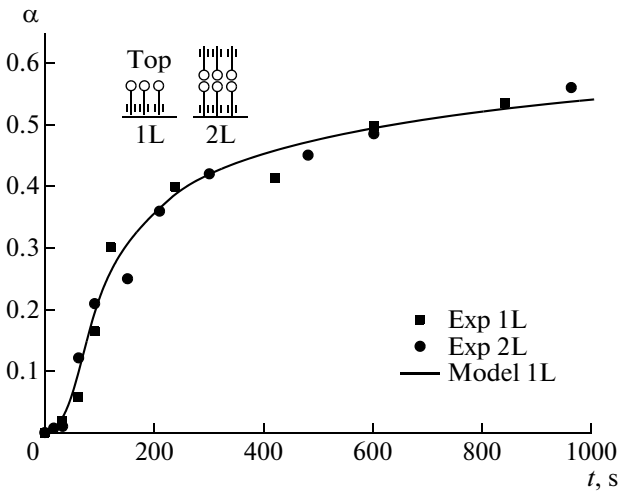

Fig. 2. Conversion (α) as a function of time (t) for the photopolymerization of the monolayer (Exp 1L) and bilayer (Exp 2L) TCA salt LB films grown at a surface pressure of $\pi = 29 \times 10^{-3}$ N/m. Orientation of the first layer of the film: the carboxyl group is far from the substrate surface (Top). The points represent experimental data, and the curve represents simulated data (Model 1L).

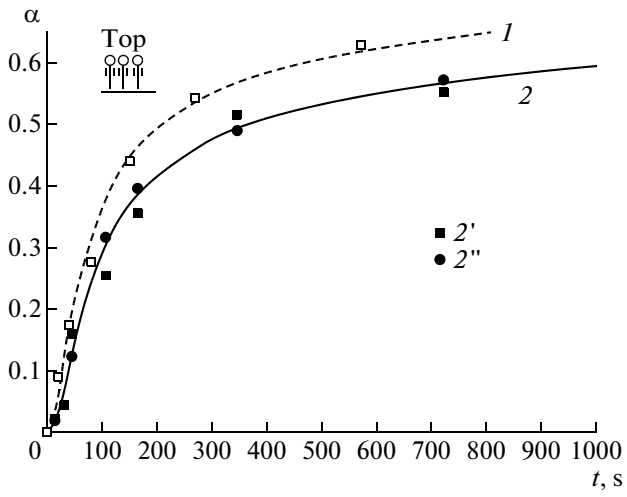

Fig. 3. Conversion $\alpha(t)$ of the monolayer (Exp 1L) DCA salt LB films grown at surface pressures of $\pi = 35 \times 10^{-3}$ (*1*) and 29×10^{-3} N/m (*2*). The points represent experimental data; (*1*, *2*) simulated data (Model 1L); (*2'*, *2"*) data of independent experiments.

salt films are presented in Fig. 4. The $\alpha(t)$ curve for the bilayer DCA salt film is well above the same curve for the monolayer film, in distinction to what is observed for the TCA salt (Fig. 2). An unexpected result is that the $\alpha(t)$ curve for the three-layer DCA salt films lies between the same curves for the monolayer and bilayer films. In order to elucidate the effect of the substrate, we grew films in which monolayers of the lead DCA salt were separated by a layer of the cadmium salt of docosanoic acid ($CdBh_2$), which has no acetylene group. The $\alpha(t)$ dependence for this mixed three-layer film is plotted in Fig. 4. Clearly, the $\alpha(t)$ curve for the three-layer DCA salt film nearly coincides with the same curve for the film with an intermediate $CdBh_2$ layer. For the monolayer DCA salt films, we studied the influence of the orientation of molecules in the layer on $\alpha(t)$ (Fig. 5). It was found that $\alpha(t)$ does depend on the orientation of molecules: for the Top orientation, the curve has a sigmoid shape; for the Bottom orientation, it has no initial flat portion. As the irradiation time is extended, the curves tend to a common saturation level. It is interesting that all TCA and DCA salt films were very stable for 1 month as they were stored under laboratory conditions. Furthermore, polymerization did not have the character of an initiated process: the IR spectra recorded immediately after irradiation coincided with the spectra recorded a week after.

POLYMERIZATION MODEL

We will accept in our model that, in a monolayer, the acetylene groups of nearest-neighbor TCA and DCA salt molecules are opposite each other, forming a two-dimensional lattice [4, 8–12]. From surface pressure (π) isotherms, we derived the area occupied by one molecule in the monolayer at $\pi = 29 \times 10^{-3}$ N/m: $S_M(\text{TCA}) = 0.204$ nm^2 and $S_M(\text{DCA}) = 0.173$ nm^2. From the same isotherms, we estimated, the intermolecular distance to be $d = 0.452$ nm for TCA and 0.416 nm for DCA.

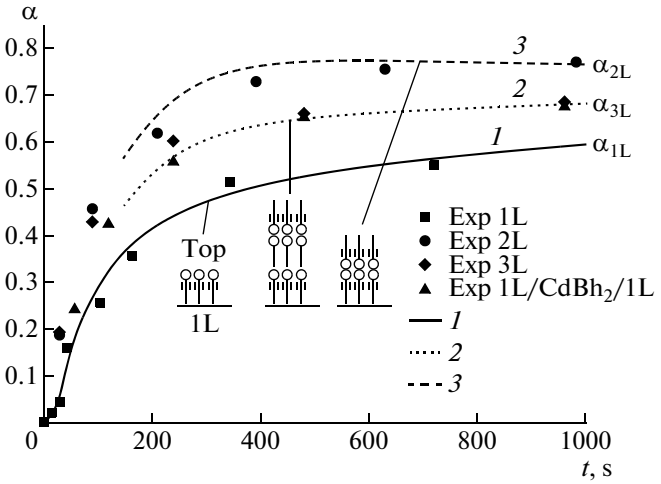

Fig. 4. Conversion $\alpha(t)$ of the monolayer (Exp 1L), bilayer (Exp 2L), and three-layer (Exp 3L) DCA salt LB films. Exp 1L/$CdBh_2$/1L —three-layer film in which two DCA salt layers are separated by a layer of the cadmium salt of docosanoic acid. The films were grown at $\pi = 29 \times 10^{-3}$ N/m. *1*, Simulated data for the monolayer film (α_{1L}); *2*, approximation of the experimental dependence for the three-layer film (α_{3L}); *3*, data estimated using the formula $\alpha_{2L} = 2\alpha_{3L} - \alpha_{1L}$.

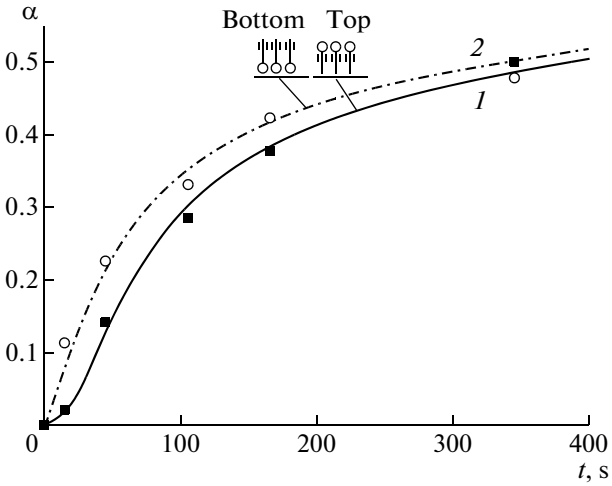

Fig. 5. Conversion $\alpha(t)$ of the monolayer (Exp 1L) of DCA salt LB films with various carboxyl group orientations relative to the substrate. *1*, Top orientation: the carboxyl group is far from the substrate surface; *2*, bottom orientation: the carboxyl group is near the substrate surface. The films were grown at $\pi = 29 \times 10^{-3}$ N/m. The points represent experimental data, and the curves represent calculated data (Model 1L).

The polymerization of the TCA and DCA salts involves the breaking of their triple bonds and the formation of C–C and C=C bonds between adjacent monomers. The length of these bonds in the polymer chain was estimated to be 0.25 nm [13]. Therefore, the polymerizing molecules come closer together. The change in the intermolecular distance (Δd) upon polymerization can be as great as $\Delta d > 0.1$ nm. For comparison, this change in diacetylenic compounds is $\Delta d = 0.0252$ nm [14, 15]. The marked difference between the Δd values for the monoacetylenic and diacetylenic compounds is likely due to the fact the monomers in polydiacetylenes are linked by the –C≡C– group [15, 16], which is longer than the C–C or C=C group bonding the monomers in polyacetylenes. The shortening of the intermolecular distance in polymerization inevitably causes marked elastic strain in the molecular structure. The Δd-based estimate of the elastic strain energy per molecule within the linear approximation with an elastic modulus of 3.7×10^3 kcal mol^{-1} nm^{-2} [5] is 0.050 eV for the diacetylenic compounds and >0.770 eV for the monoacetylenic compounds. Under the assumption that the elastic strain energy is equal to the activation energy of spontaneous polymerization [5, 17], the difference between the elastic strain energy values provides an explanation of the fact that the diacetylenic compounds can spontaneously polymerize at room temperature, while the monoacetylenic compounds are stable upon long storage. The reactive groups in the monoacetylenic compounds cannot come sufficiently close together. As a consequence, polymerization occurs only under UV irradiation. It is assumed that there is a photoexcited state in which the TCA or DCA molecule can react with an adjacent molecule. Polymerization generates free valences. We found that polymerization is not initiating in character; that is, the free valence of the polymer chain cannot react with an adjacent molecule. The assumption that the free valences are not involved in polymerization implies that only dimer formation should take place. Under this assumption, the polymerization process would be similar to two-site adsorption and the formation of a dimer would be similar to the adsorption of a diatomic molecule. If this were the case, the kinetics of the process would be describable by the same equations as the kinetics of two-site adsorption [18]. However, we failed to fit the polymerization kinetics to the kinetic equation of two-site adsorption. Therefore, the polymerization process is not limited to dimer formation. This is possible when the free valence of the polymer chain can react with a photoexcited molecule. Thus, we accept in our model that only photoexcited molecules are involved in polymerization.

In the topochemical polymerization of diacetylenic compounds, the polymer chain growth direction is determined by the crystal structure of the polymerizing compound [6, 19] and by the admissible angles between the covalent bonds of the carbon atoms in the chain. In monoacetylenic compounds, only photoexcited molecules are active, whose structure is unknown. Moreover, polymerization brings about substantial structural strain in the molecules. For these reasons, we will ignore the specific crystallographic features of the molecular packing in the film and will consider only two structure parameters, namely, the number of neighbors around each photoexcited molecule (Z) and the surface area per molecule in the layer.

We will consider a monolayer LB film exposed to a UV photon beam. The photons are absorbed with some probability to produce photoexcited molecules. The photoexcitation rate B (number of photoexcited molecules forming in the monolayer in 1 s per monolayer molecule) is

$$B = (1 - \alpha)\Phi S_M \eta,$$

where Φ is the photon flux and η is the quantum yield of the photoexcitation of the molecule. The photoexcited molecule interacts with its closest environment (free valence of the polymer chain or an unexcited molecule) with some probability $P_S(z)$. The calculation of the probability $P_S(z)$ is described in the Appendix. The photopolymerization rate per molecule of the monolayer is $w = BP_S(z)$.

For an arbitrary point of time, the kinetic equation is written as

$$\frac{\partial \alpha}{\partial t} = w.$$

By numerical integration of this equation subject to the initial condition $\alpha(t = 0) = 0$, we obtained the kinetic relationships $\alpha(t)$. Here, Φ and S_M are experimental parameters. The other parameters of the model—Z, N_0, P_{N0}, P_{C0}, m, and η (see Appendix)—were fitted so as to minimize the deviation between the experimental data points and the calculated curves.

DISCUSSION

The $\alpha(t)$ curve for the TCA salt is a sigmoid tending to saturation at the $\alpha \approx 0.6$ level (Fig. 2). An analysis of the influence of the model parameters P_{C0} and P_{N0} on the shape of the $\alpha(t)$ curve demonstrated that the sigmoidality takes place when the probability of dimer formation (i.e., chain initiation) is well below the probability of the addition of the photoexcited molecule to the polymer chain: $P_{C0} \ll P_{N0}$. Hence, it can be assumed that, at the early stages of irradiation, dimers accumulate in the layer and the initial portion of the $\alpha(t)$ curve is flat because of the low probability P_{C0}. After dimer accumulation, the polymerization rate is determined by the chain propagation rate, which is governed by the probability P_{N0}. The model calculation demonstrates that the average oligomer consists of $N = 7$ units and the number of neighbors is $Z = 4$ (square lattice), $P_{C0} = 5 \times 10^{-4}$, $P_{N0} = 0.85$, the quantum yield of photoexcitation is $\eta = 0.03$, and $m = 7$. The coincidence of the experimental $\alpha(t)$ curves for

the monolayer and bilayer films (Fig. 2) indicates that each layer polymerizes independently and that the effect of the substrate can be neglected.

The model calculations (Fig. 3) show that, as compared to the TCA salt, the DCA salt is characterized by a higher probability of its excited molecule interacting with unpolymerized neighbors ($P_{C0} = 2 \times 10^{-3}$) and by a smaller value of the parameter m ($m = 6$). The other parameters of the model— N, Z, P_{N0}, and η—are the same as for the TCA salt. The fourfold increase in P_{C0} causes the disappearance of the initial flat portion of the $\alpha(t)$ curve. The higher probability of dimer formation and the smaller m value for the DCA salt are possibly due to the fact that the reactive acetylene group in this salt is near the carboxyl group, which likely determines the position of the molecule in the layer. Because of this, the plane of carboxyl groups is more ordered than the plane of hydrocarbon tails and the probability P_{C0} for the DCA salt (in which the triple bond is near the carboxyl group) is higher than the same probability for the TCA salt.

The ordering of a monolayer in film formation depends considerably on the surface pressure π [20]. Raising π for the DCA salt to 35×10^{-3} N/m, above which the film undergoes collapse, indeed increases the salt conversion in the monolayer (Fig. 3). The model calculations suggest that this change in the $\alpha(t)$ curve can be explained by the increase in the number of neighbors to $Z = 6$, by the increase in the mean oligomer length to nine units, and by the decrease in the parameter m to 5; that is, raising the surface pressure in film formation likely changes the molecular packing in the layer. This change in the molecular packing would be expected to alter the shape of the surface pressure isotherm; however, no change in the isotherm was observed in fact.

For the DCA salt, we observed a substantial difference between the salt conversions in the monolayer and bilayer films. This can be due to the effect of the substrate or the interaction between carboxyl groups from adjacent layers. In order to decide between these two possibilities, we grew a film in which two DCA salt monolayers were separated by a $CdBh_2$ monolayer. If the difference between the $\alpha(t)$ curves for the monolayer and bilayer were due to the effect of the substrate on the first layer, the α_{2L} and α_{3L} curves would coincide (Fig. 4). In fact, the α_{3L} curve lies between α_{1L} and α_{2L}.

We found that, if the initial portions of the $\alpha(t)$ curves ($\alpha(t < 150$ s)) are left out of consideration, the following relationship will be true: $\alpha_{2L} \approx 2\alpha_{3L} - \alpha_{1L}$. It is likely that the DCA salt molecules in the bilayer are ordered more perfectly than those in the monolayer owing to the interlayer interaction of carboxyl groups. Therefore, the three-layer film can be viewed as consisting one monolayer and one bilayer. Under the assumption that the salt conversion for the monolayer is $\alpha(t) = \alpha_{1L}$ and the salt conversion for the bilayer is $\alpha(t) = \alpha_{2L}$, the conversion for the three-layer film is $\alpha_{3L} = (\alpha_{1L} + \alpha_{2L})/2$, and this was actually observed experimentally.

At the same time, replacing the DCA layer in the bilayer with a layer of $CdBh_2$ molecules (which have no triple bond) does no change the conversion of the bilayer (Fig. 4). This finding proves that it is the interlayer interaction of carboxyl groups that affects the coordination of molecules in the bilayer. Thus, the fact that the salt conversion in the bilayer is higher than that in the monolayer is mainly due to the interaction between carboxyl groups from the adjacent layers. The triple bond in the TCA molecule, as distinct from that in the DCA molecule, is far from the carboxyl group. As a consequence, the interlayer interaction of carboxyl groups in the case of TCA exerts only a weak effect on the orientation of the triple bonds and does not lead to any difference between the salt conversions in the monolayer and bilayer (Fig. 2).

If the DCA salt molecules are reoriented from the Top orientation to the Bottom orientation, a substrate effect will be observed for the initial portion of the $\alpha(t)$ curve (Fig. 5). The model calculations demonstrate that the dimer formation probability for the Bottom orientation ($P_{C0} = 1 \times 10^{-2}$) is 5 times higher than the same probability for the Top orientation (2×10^{-3}). The other parameters of the model are the same in both cases. After the formation of a sufficient amount of the dimers, the polymerization rate is determined by chain propagation and, accordingly, the two $\alpha(t)$ dependences tend to approximately the same saturation level.

CONCLUSIONS

The photopolymerization of thin LB films (1–3 layers) of the lead salts of TCA and DCA has been investigated. A kinetic model has been constructed for the two-dimensional polymerization of the monoacetylenic compounds. The basic assumption of this model is that only photoexcited molecules are involved in polymerization. The model $\alpha(t)$ relationships provide a good fit to the observed curves. It was found experimentally that the $\alpha(t)$ dependences for TCA salt monolayer and bilayer are nearly the same. This indicates that the polymerization processes in adjacent TCA salt layers are fairly independent. Conversely, the extent of polymerization of the DCA salt in the bilayer film is higher than is observed in the monolayer film. A test experiment involving an intermediate $CdBh_2$ layer demonstrated that the interlayer interaction of carboxyl groups favors the spatial ordering of molecules in the bilayer and thus increases the DCA salt conversion in the bilayer over the conversion in the monolayer. It is assumed that the large α values of up to 0.85, observed for thick films containing 20 LB layers or more [3], are due to the formation of bilayers through the interlayer coordination of carboxyl groups. The effect of the substrate on the photopoly-

merization of monolayer films was studied. It was deduced that the dimer formation rate for the DCA salt with the Bottom orientation of molecules relative to the substrate is 5 times higher than in the case of the Top orientation. The value of conversion increases with an increasing surface pressure π. Simulations demonstrated that, as π is increased, the number of neighbors of a molecule in the film increases from 4 to 6. An analysis of experimental data in terms of the model suggests that the observed saturation of the $\alpha(t)$ dependences for the TCA and DCA salts at the α = 0.5–0.6 level can be explained by the lengthening of the average intermonomer distance in the layer during polymerization.

APPENDIX

Figure 6 shows the possible configurations and arrangements of molecules around an excited molecule (*b*) in a monolayer. The case of eight neighbors ($Z = 8$) is depicted. The neighbors may be unpolymerized molecules (*a*) or monomers of the polymer chain (*c*). Clearly, there can be $Z + 1$ variants differing in the number of neighbor monomers (*c*): $\xi = 0 - Z$. In each variant, the number of configurations (k_ξ) is equal to the number of combinations C_Z^ξ:

$$k_\xi = C_Z^\xi = \frac{Z!}{(Z-\xi)!\xi!}. \quad \text{(A.1)}$$

The probability that an arbitrarily chosen molecule in the layer is an unpolymerized molecule is $(1 - \alpha)$, where α is the conversion of the layer. The probability that a photoexcited molecule is surrounded only by unpolymerized molecules ($\xi = 0$ configuration), $P_U(\xi)$, is

$$P_U(0) = (1-\alpha)^8 k_0.$$

The probability that this molecule is surrounded by one monomer and seven unpolymerized molecules is

$$P_U(1) = (1-\alpha)^7 \alpha^1 k_1.$$

Likewise, the probability that this molecule is surrounded by ξ monomers and $(Z - \xi)$ unpolymerized molecules is

$$P_U(\xi) = (1-\alpha)^{z-\xi}\alpha^\xi k_\xi. \quad \text{(A.2)}$$

Each polymer chain has two free valences. The length of polymer chains increases with increasing α. We assume that the mean length of the polymer chain (N) depends on the conversion of the layer:

$$N = 2 + N_0\alpha, \quad \text{(A.3)}$$

where $N_0\alpha(t \to \infty)$ is the mean number of new units added to the dimer at the polymerization time $t \to \infty$. For an arbitrary monomer, the probability that this monomer will be terminal in the polymer chain (will have a free valence) is, obviously, equal to

$$\gamma = 2/N. \quad \text{(A.4)}$$

A photoexcited molecule can participate in polymerization by adding to the polymer chain, if there is a polymer chain end (monomer with a free valence) among its nearest neighbors, or by interacting with an adjacent unpolymerized molecule. Let the probability of the addition of the photoexcited molecule to the end of the polymer chain be designated P_N and the probability of the interaction of this molecule with an unpolymerized molecule be designated P_C. Obviously, these probabilities depend on the mean intermolecular distance. If polymerization is accompanied by local compression of the layer in the places of the formation of the polymer chain, then the layer will expand outside the polymer chains because of the elastic stress. With increasing α, the distance between unpolymerized molecules should increase and the probabilities P_N and P_C should decrease. In the model considered, this effect is taken into account by multiplying P_N and P_C by the factor $(1 - \alpha)^m$:

$$P_N = P_{N0}(1-\alpha)^m, \quad \text{(A.5)}$$

$$P_C = P_{C0}(1-\alpha)^m, \quad \text{(A.6)}$$

where P_{N0} and P_{C0} are the probabilities of the interaction of the photoexcited molecule with the end of the polymer chain and with an unpolymerized molecule in a weakly polymerized layer ($\alpha \approx 0$), respectively, and m is the exponent determining the rate at which the

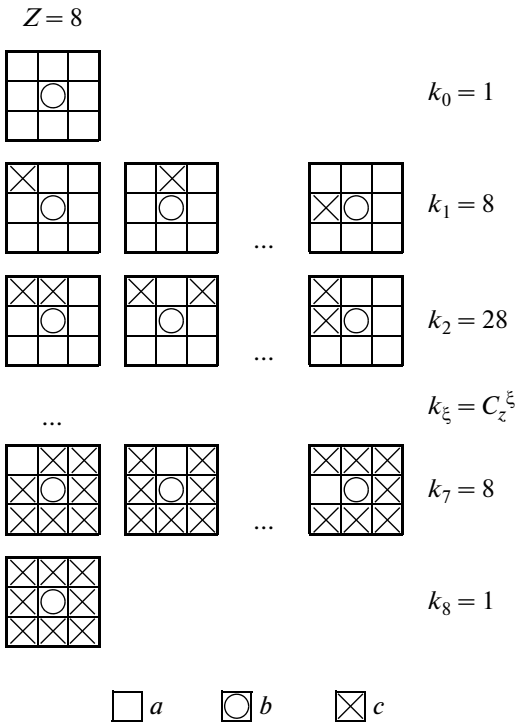

Fig. 6. Possible arrangements of neighbors around a photoexcited molecule (*b*) in the monolayer (top view of the surface). The monolayer is filled with (*a*) unpolymerized molecules and (*c*) polymerized molecules (monomer units of the polymer chain). Z is the number of neighbors, and k_ξ is the possible number of configurations with ξ polymerized neighbor molecules.

probabilities decrease with an increasing intermolecular distance.

Using the rule of combination of logically related events, we will find the probability of the interaction of the photoexcited molecule with a neighbor in the configurations in which there are ξ monomers and $(Z-\xi)$ unpolymerized molecules $P_K(\xi)$:

$$P_K(\xi) = 1 - (1 - P_C)^{z-\xi}(1 - P_N\gamma)^{\xi}. \quad \text{(A.7)}$$

The probability of interaction in the configurations in which there are ξ monomer neighbors with account taken of the probability of appearance of these configurations, $P_U(\xi)$, is

$$P_R(\xi) = P_K(\xi)P_U(\xi) = (1 - (1 - P_C)^{z-\xi} \times (1 - P_N\gamma)^{\xi})(1 - \alpha)^{z-\xi}\alpha^{\xi}k_{\xi}. \quad \text{(A.8)}$$

Using the rule of combination of logically related events again, we find that the total probability of the interaction of the photoexcited molecule with a neighbor in all possible configurations is

$$P_S(z) = 1 - \prod_{\xi=0}^{z}(1 - P_R(\xi)). \quad \text{(A.9)}$$

ACKNOWLEDGMENTS

The authors are grateful to A.S. Medvedev for IR spectroscopic measurements and to L.L. Sveshnikova for helpful recommendations and remarks.

REFERENCES

1. Guillet, J., *Polymer Photophysics and Photochemistry*, Cambridge: Cambridge Univ. Press, 1985.
2. Badmaeva, I.A., Sveshnikova, L.L., Repinskii, S.M., Koltunov, K.Yu., Shvartsberg, M.S., Shergina, S.I., Zanina, A.S., and Yanusova, L.G., *Zh. Fiz. Khim.*, 2001, vol. 75, no. 12, p. 2256 [*Russ. J. Phys. Chem.* (Engl. Transl.), vol. 75, no. 12, p. 2069].
3. Badmaeva, I.A., Nenasheva, L.A., Polovinkin, V.G., Repinsky, S.M., and Sveshnikova, L.L., *Thin Solid Films,* 2004, vols. 455–456, p. 557.
4. Sveshnikova, L.L., Badmaeva, I.A., Dembo, K.A., and Yanusova, L.G., *Kristallografiya*, 2005, vol. 50, no. 5, p. 920 [*Crystallogr. Rep.* (Engl. Transl.), vol. 50, no. 5, p. 854].
5. Baughman, R.H., *J. Chem. Phys.*, 1978, vol. 68, no. 7, p. 3110.
6. Menzel, H., Horstmann, S., Mowery, M.D., Cai, M., and Evans, C.E., *Polymer*, 2000, vol. 41, no. 22, p. 8113.
7. Milekhin, A., Friedrich, M., Hiller, K., Wiemer, M., Gessner, T., and Zahn, D.R., *J. Vac. Sci. Technol., B*, 1999, vol. 17, no. 4, p. 1733.
8. Pingsheng, H., Huilin, Z., and Gang, Z., *Polymer*, 2003, vol. 44, no. 11, p. 3235.
9. Klechkovskaya, V.V. and Feigin, L.A., *Kristallografiya*, 1998, vol. 43, no. 6, p. 975 [*Crystallogr. Rep.* (Engl. Transl.), vol. 43, no. 6, p. 917].
10. Schwartz, D.K., *Surf. Sci. Rep.*, 1997, vol. 27, nos. 7–8, p. 245.
11. Dupres, V., Cantin, S., and Perrot, F., *J. Chem. Phys.*, 2002, vol. 116, no. 9, p. 3822.
12. Peng, J.B., Foran, G.J., Barnes, G.T., and Gentle, I.R., *J. Chem. Phys.*, 2005, vol. 123, p. 214705.
13. Dultsev, F.D., *Sens. Actuators, B*, 2008, vol. 129, no. 1, p. 171.
14. Bloor, D., Koski, L., Stevens, G.C., Preston, F.H., and Ando, D.J., *J. Mater. Sci.*, 1975, vol. 10, p. 1678.
15. Wegner, G., *Makromol. Chem.*, 1971, vol. 145, p. 85.
16. Tieke, B., Graf, H-J., Wegner, G., Naegele, B., Ringsdorf, H., Banerjie, A., Day, D., and Lando, J.B., *Colloid Polym. Sci.*, 1977, vol. 255, no. 6, p. 521.
17. Santoro, M., Ciabini, L., Bini, R., and Schettino, V., *J. Raman Spectrosc.*, 2003, vol. 34, p. 557.
18. Hayward, D.O. and Trapnell, B.M.W., *Chemisorption*, London: Butterworths, 1964, p. 92.
19. Wegner, G., *Pure Appl. Chem.*, 1977, vol. 49, p. 443.
20. Gericke, A. and Huhnerfuss, H., *Thin Solid Films*, 1994, vol. 245, nos. 1–2, p. 74.